Available online at www.sciencedirect.com
SCIENCE DIRECT®
Catalysis Today 88 (2004) 139–151
CATALYSIS TODAY
www.elsevier.com/locate/cattod

Hydrodehalogenation with sonochemically prepared Mo_2C and W_2C

James D. Oxley, Millan M. Mdleleni, Kenneth S. Suslick*

School of Chemical Sciences, University of Illinois at Urbana-Champaign, 600 S. Mathews Ave., Urbana, IL 61801, USA

Abstract

The catalytic hydrodehalogenation (HDH) of several halogenated organic compounds was performed over sonochemically prepared molybdenum carbide and tungsten carbide at low temperatures ($T = 200–300\,^{\circ}C$). Both catalysts were selective, active, and stable for all substrates tested. Benzene was observed as the major product for the HDH of fluoro-, chloro-, bromo- and iodobenzene, with activities following the trend of $C_6H_5F > C_6H_5Cl > C_6H_5Br > C_6H_5I$. For the HDH of chlorofluorocarbons (CFCs), Cl was selectively removed over F and alkanes were the major product. In the liquid phase, the HDH of polychlorinated and polybrominated biphenyls resulted in biphenyl as the only product. The HDH of substrates bearing aliphatic C–Cl bonds occurs faster than those with arene C–Cl bonds. Time-on-stream studies of HDH of chlorobenzene show high stability for the sonochemically prepared catalysts, with half-lives as long as 600 h.

Keywords: Hydrodehalogenation; CFC; Catalysts; PCB; Molybdenum; Tungsten; Carbide

1. Introduction

The environmental impact of halogenated organics has led to the strict regulation of halocarbons. Widespread use of chlorofluorocarbons (CFCs) has contributed to both global warming and depletion of the ozone layer [1]. Meanwhile, the use of polychlorinated biphenyls (PCBs) and their brominated analogues (PBBs) has resulted in their global bioaccumulation and environmental contamination [2–5]. Additional environmental and health hazards stem from the use of various other halogenated organics including chlorophenols, chlorobenzenes, and 1,1,1-trichloro-2,2-bis(*p*-chlorobiphenyl)ethane (DDT). The remediation of contaminated sites, disposal of existing halogenated organics, and the prevention of future pollution is a serious problem that requires new solutions.

There are several approaches to the remediation of halocarbons: activated carbon adsorption, thermal incineration, catalytic oxidation, and hydrodehalogenation (HDH) [6]. While treatment with activated carbon can aid in the recovery and recycling of halogenated solvents, it is not a viable method for destruction of halocarbons. Thermal incineration ($\geq 900\,^{\circ}C$) is successful at destroying halogenated organics, however, the presence of oxygen during the process can lead to the formation of even more toxic secondary pollutants such as polyhalogenated dioxins and furans [7–11]. Emissions from incineration plants are a major contributor to the 3000 kg of polyhalogenated dioxins and furans produced every year [12]. Catalytic oxidation allows for the use of lower temperatures ($<600\,^{\circ}C$), but current catalysts have relatively low activity [6,13].

* Corresponding author.

0920-5861/$ – see front matter
doi:10.1016/j.cattod.2003.11.010

Catalytic HDH of halogenated organics produces non-halogenated organic compounds at lower temperatures (<300 °C) and is the most promising of the remediation techniques available. Current technology for HDH, however, is severely limiting. Previous HDH studies have focused on the noble metals Pd, Pt, and Rh; unfortunately, these are also excellent hydrogenation catalysts, so their selectivity for HDH is poor. For example, the HDH of chlorobenzene over Pd- or Pt-based catalysts leads to substantial production of chlorocyclohexane and cyclohexane [14]. Furthermore, it has been reported that these catalysts are prone to deactivation by attack from the HCl produced during the course of HDH and by coke formation [15–19]. The use of Ni has proven to be more selective and stable than Pd and Pt, but its activity is lower [20–22]. Conventionally prepared Mo- and W-based catalysts have exhibited similar activity and stability for the HDH of CFCs, but are difficult to prepare with high surface area and have not been examined with other halogenated organics [23,24].

The development of sonochemistry as an important new technique for the synthesis of nanostructured inorganic materials has only recently been established [25–28]. Sonochemistry occurs in liquids subjected to intense ultrasonic irradiation and derives from localized hotspots formed by the implosive collapse of micron-sized bubbles during acoustic cavitation [29,30]. Our group has previously developed the sonochemical synthesis of high surface area, nanostructured molybdenum carbide (Mo_2C) and examined its catalytic dehydrogenation activity [31].

As part of ongoing studies in this laboratory of heterogeneous catalysis by sonochemically prepared catalysts, the activity, selectivity, and stability of sonochemically prepared Mo_2C and W_2C were examined for the HDH of halogenated organics. Monohalobenzenes were tested as substrates due to their close resemblance to moieties found in common pesticides, herbicides, disinfectants, and flame-retardants. Dichlorodifluoromethane (CFC-12) was used as a HDH model substrate for CFCs, and 4,4′-dichlorobiphenyl was used as a model substrate for PCBs. In this paper we report on the HDH rates of several halogenated hydrocarbons over sonochemically prepared Mo_2C and W_2C catalysts.

Sonochemical preparation of nanophase materials arises from acoustic cavitation: the formation, growth, and implosive collapse of bubbles in a liquid irradiated with high intensity ultrasound [25,32]. The collapse of such bubbles creates hot spots with temperatures as high as 5000 K, pressures of hundreds of atmosphere, and cooling rates in excess of 10^{10} K/s [30,33]. These conditions provide an unusual method for the decomposition of organometallics and the consequential sonochemical formation of nanostructured materials [26,31,32]. For our purposes, $Mo(CO)_6$ and $W(CO)_6$ were used for the formation of Mo_2C and W_2C, respectively.

2. Experimental

2.1. Materials and equipment

Unless otherwise noted, all synthesis, preparation, and handling of the materials were carried out in an Ar atmosphere box (vacuum atmospheres) with <0.5 ppm O_2. Pentane was dried and distilled over Na/benzophenone and degassed prior to use. Hexadecane (Aldrich, 99%) and decane (Aldrich, 99%) were dried and distilled over Na and degassed. All halogenated hydrocarbons (>99%), except the CFCs and PCBs, were purchased from Aldrich and used as received. Dichlorodifluoromethane (CFC-12) was obtained from Mattex Service Company (Champaign, IL) and chlorodifluoromethane (CFC-22) was purchased from S.J. Smith. Methane (99.99%), hydrogen (99.99%), and helium (99.9%) were purchased from S.J. Smith and further purified by passing through Oxytraps (Agilent) prior to use. The polyhalogenated biphenyls and diphenylethers were obtained from the Marvel Storeroom (University of Illinois at Urbana-Champaign) and used as received. $Mo(CO)_6$ (98%) and $W(CO)_6$ (99%) were purchased from Strem and used without further purification. LiOH (Laboratory Grade, Fisher) and alumina (neutral 150 mesh, Aldrich) were heat treated at 200 °C under vacuum for 24 h to remove adsorbed water. All sonications were done at 20 kHz using a Sonics & Materials VCX600 with a 1 cm^2 titanium horn at an acoustic intensity of ~60 W cm^{-2} in a glass vessel under Ar atmosphere.

Reactions with the CFCs and chloroalkanes were analyzed with a 5730A Hewlett-Packard gas chromatograph (GC) fitted with a flame ionization detector and a quadrupole mass spectrometer (Spectra Instru-

ments). Separations were carried out with a 10% Carbowax 20M on Chromosorb W-HP packed column or an *n*-octane Porasil C packed column. All other reactions were analyzed with a Hewlett-Packard 6890 GC system equipped with an HP-5973 Mass Selective Detector and a DB-35MS column (HP-GCMS).

2.2. Preparation of catalysts

Nanostructured Mo_2C was prepared as previously described [31]. A slurry of 2.0 g $Mo(CO)_6$ in 35 ml hexadecane was sonicated for 3 h at 80 °C under argon. The resulting black powder was filtered and washed several times with pentane. The washed powder was then heated to 100 °C for 12 h under vacuum to remove unreacted $Mo(CO)_6$. Oxygen contamination was removed by heating the amorphous product at 500 °C for 12 h under a 1:1 flow of CH_4:H_2 at 30 cm^3/min. Elemental analysis of the treated powder gives a Mo/C ratio of 1.97. The W_2C was prepared in a similar manner with $W(CO)_6$ as the starting material. Elemental analysis of the treated powder gives a W/C ratio of 2.13.

2.3. Gas/vapor phase HDH

Gas/vapor catalytic studies were performed at atmospheric pressure with 100 mg of catalyst in a single-pass quartz microreactor. Vapors of liquid substrates were carried from a thermally equilibrated saturator by a flow of purified H_2 and He. Flow rates (27.5 cm^3/min) were controlled with digital mass-flow controllers (MKS). All vapors passed through a LiOH plug prior to entering the online HP-GCMS.

2.4. Liquid phase HDH

The liquid phase HDH experiments were carried out using a custom-built stainless steel pressure vessel equipped with a sample withdrawal system [27]. The catalyst (50 mg) was dispersed in 50 ml of decane containing 0.1 M substrate. The vessel was flushed with H_2 and pressurized to 500 psi with H_2. For consistency, t_0 was denoted as the time when the target temperature was reached. Samples were removed periodically throughout each experiment. The sampling system was equipped with a 2 μm stainless steel filter to prevent removal of catalyst from the system. Aliquot size was approximately 0.25 ml. The samples were then centrifuged to remove any particulates, diluted 1:10 with pentane, and analyzed with GC–MS.

2.5. Characterization

X-ray powder diffraction (XRD) patterns were recorded on a Rigaku D-max diffractometer using Cu Kα radiation. X-ray photoelectron spectra (XPS) were collected on a Phi-540 spectrometer using Mg Kα radiation and were referenced to the carbidic C (282.7 eV) peak. Scanning and transmission electron micrographs (SEM and TEM, respectively) were taken on Hitachi S800 and Philips CM-12 electron microscopes operated at 20 and 120 kV, respectively. Surface areas of the sonochemically prepared catalysts were determined by Brunauer–Emmet–Teller (BET) N_2 adsorption isotherms at 77 K.

3. Results and discussion

3.1. Catalyst characterization

The XRD pattern of the sonochemically prepared Mo_2C is characteristic of poorly crystalline Mo_2C. It exhibits broad peaks centered at d-spacings of 2.39, 1.48, and 1.28 Å which correspond to the [1 1 1], [2 2 0], and [3 1 1] reflections of the face centered cubic Mo_2C (2.38, 1.47, and 1.26 Å), respectively [34]. Similarly, the XRD pattern for the sonochemically prepared W_2C exhibits broad peaks centered at d-spacings of 2.37, 1.48, and 1.26 Å, which correspond to the [1 1 1], [2 2 0], and [3 1 1] reflections of the face centered cubic WC_{1-x} (2.38, 1.47, and 1.26 Å), respectively [35]. The apparent asymmetry of the [1 1 1] reflection may be do to overlap with the [2 0 0] reflection. An average crystallite size of 2.0 nm for Mo_2C and 1.8 nm for W_2C were estimated from the application of the Scherrer equation to the width of the [2 2 0] and [3 1 1] reflection of each pattern [36]. Scanning and transmission electron micrographs, Fig. 1, reveal that the material exists as a porous agglomeration of clusters of spherical particles with an average diameter of ∼3 nm, consistent with the X-ray diffraction line widths. The surface area before heat treatment was 188 and 120 m^2/g for Mo_2C and W_2C,

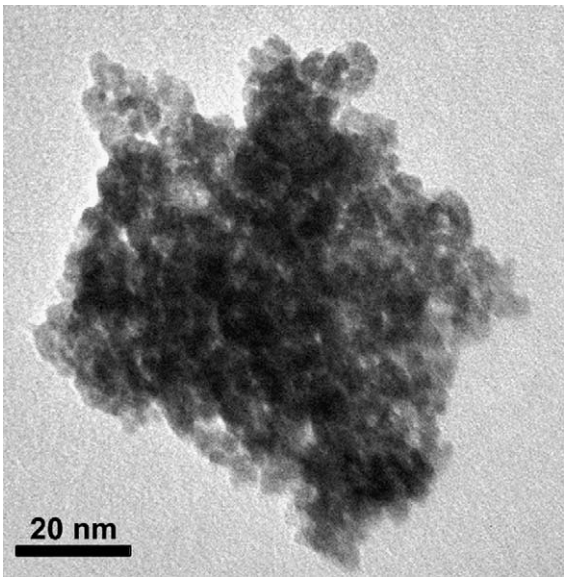

Fig. 1. TEM of sonochemically prepared Mo_2C.

respectively. Following heat treatment, the surface areas were reduced to 130 and 60 m^2/g, respectively.

The XPS spectrum of the sonochemically prepared Mo_2C shows a well-defined spin-coupled Mo ($3d_{5/2}$, $3d_{3/2}$) doublet at respective binding energies of 227.4 and 230.5 eV with a $d_{5/2}/d_{3/2}$ area ratio of 1.5. Characteristic of Mo_2C, the carbidic C1s peak was observed at a binding energy of 283.5 eV [37]. The XPS spectrum of sonochemically prepared W_2C shows a well-defined spin-coupled W ($4f_{7/2}$, $4f_{5/2}$) doublet at respective binding energies of 31.2 and 33.2 eV with an $f_{7/2}/f_{5/2}$ ratio of 1.33. The carbidic C1s peak was observed as a broad peak at a binding energy of 284.3 eV.

3.2. Gas–solid catalytic HDH activity

The HDH of aryl halides was used to investigate the general selectivity, stability, and activity of sonochemically prepared Mo_2C and W_2C. The activity results are summarized in Table 1. The HDH of chlorobenzene over W_2C, shown in Fig. 2, leads exclusively to benzene. Neither chlorocyclohexane nor cyclohexane was observed under any conditions. This demonstrates the higher selectivity of the sonochemically prepared Mo_2C for HDH of chlorobenzene compared to the commonly used catalysts based on Pd, Pt and Rh [15–17]. Lee et al. [38] reported that conventional Mo_2C catalyzes the hydrogenation of benzene to cyclohexane. Despite the high H_2 ratio to substrate ratio (typically 200:1) used in these studies, however, we observed *no hydrogenation products* during the HDH of aromatics over Mo_2C or W_2C. Thus, it can be concluded that the hydrogenation of benzene is completely suppressed under HDH conditions. Reducing the H_2/substrate ratio to 1:10 resulted in a 53% decrease in rate to 2.7×10^{17} molecules $g^{-1}\,s^{-1}$, but no change in selectivity. A similar trend was observed for the HDH of chlorobenzene with Mo_2C as the temperature and H_2/substrate ratios were varied.

Table 1
HDH activity of substrates[a]

Substrate	Activity ($\times 10^{17}$)	Catalyst
Fluorobenzene	4.5×10^{17}	W_2C
	6.5×10^{17}	Mo_2C
Chlorobenzene	5.2×10^{17}	W_2C
	3.7×10^{17}	Mo_2C
Bromobenzene	4.3×10^{17}	W_2C
	1.7×10^{17}	Mo_2C
Iodobenzene	1.0×10^{17}	W_2C
	0.3×10^{17}	Mo_2C
m-Dichlorobenzene	8.0×10^{16}	Mo_2C
m-Chlorotoluene	3.8×10^{17}	Mo_2C
Chlorocyclohexane	3.6×10^{18}	Mo_2C
1-Chlorobutane	1.7×10^{18}	Mo_2C
1-Chloropropane	1.3×10^{18}	Mo_2C
2-Chloropropane	4.0×10^{18}	Mo_2C
p-Chloro-α,α,α-trifluorotoluene	4.0×10^{17}	Mo_2C
p-Chlorofluorobenzene	6.0×10^{17}	Mo_2C
α,α,α-Trifluorotoluene	1.5×10^{18}	Mo_2C
p-Fluorotoluene	6.8×10^{17}	Mo_2C
Hexafluorobenzene[b]	5.1×10^{17}	Mo_2C
	2.7×10^{17}	W_2C
Dichlorodifluoromethane	1.6×10^{19}	Mo_2C
Difluorochloromethane	3.2×10^{18}	Mo_2C
Tetrachloroethylene	4.3×10^{17}	Mo_2C
4,4′-Dichlorobiphenyl	1.7×10^{18}	Mo_2C
	2.2×10^{18}	W_2C
	1.4×10^{18}	W_2C (air)
Polychlorinateddiphenylether	2.2×10^{18}	W_2C
4,4′-Dibromodiphenylether	3.0×10^{18}	W_2C
4,4′-Dibromobiphenyl	2.9×10^{20}	W_2C
	6.6×10^{19}	Mo_2C
Pentachlorophenol	2.4×10^{20}	W_2C
Trichlorophenol	2.8×10^{18}	W_2C
DDT	1.8×10^{17}	W_2C

[a] All activities measured at 300 °C after 2 h of catalysis.
[b] Activity measured at 350 °C.

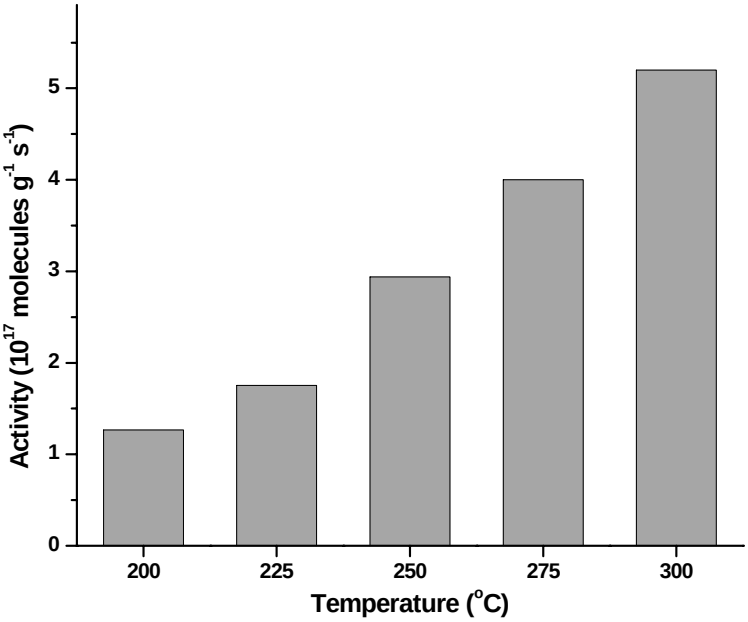

Fig. 2. Catalytic activity of W_2C for the HDH of chlorobenzene. Conditions: $P_{H_2}/P_{substrate} = 200{:}1$ and space velocity $= 16{,}500\,h^{-1}$.

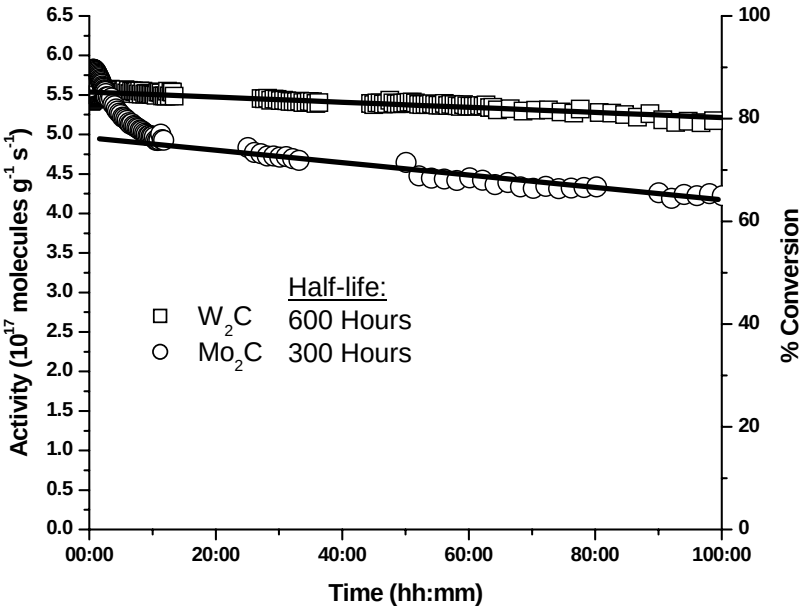

Fig. 3. Stability of Mo_2C and W_2C for the HDH of chlorobenzene. Conditions: 300 °C, $P_{H_2}/P_{substrate} = 200{:}1$ and space velocity $= 16{,}500\,h^{-1}$.

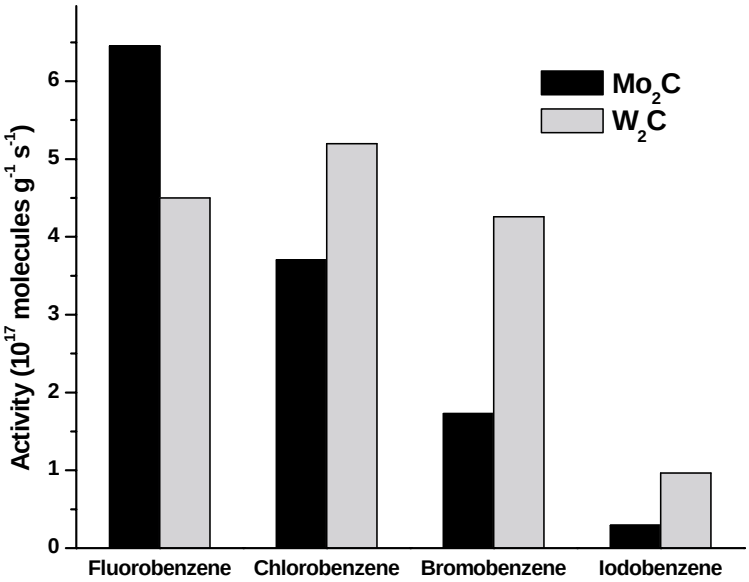

Fig. 4. Catalytic activity for the HDH of halobenzenes with Mo_2C and W_2C. Conditions: 300 °C, $P_{H_2}/P_{substrate}$ = 200:1, and space velocity = 16,500 h^{-1}.

The stability of sonochemically prepared Mo_2C and W_2C catalysts during the HDH of chlorobenzene was investigated at 300 °C. As shown in Fig. 3, no significant deactivation of the catalyst was observed with increasing time-on-stream. Following 100 h of continuous exposure of the catalysts to the reaction mixture, the rates decreased by a modest margin of ∼15%. This decrease in activity allows for a half-life estimation of 300 and 600 h for the HDH of chlorobenzene with Mo_2C and W_2C, respectively.

In addition to chlorobenzene, the HDH of fluorobenzene, bromobenzene and iodobenzene was investigated. As shown in Fig. 4, the catalysts are active at ambient pressure and low temperatures for all four substrates. The HDH of aryl halides produces exclusively benzene, with no hydrogenation observed. The activities over Mo_2C follow the unusual pattern of $C_6H_5F > C_6H_5Cl > C_6H_5Br > C_6H_5I$. With the exception of C_6H_5F, the activity of W_2C follows the same pattern and is greater than Mo_2C. These results follow a similar trend observed with Ni HDH catalysts, and suggest a mechanism involving the electrophilic attack of hydrogen on the adsorbed halobenzene [39–41]. The rate is governed by the electron affinity of the halogen and its effect on the halogen's ability to interact with the catalyst surface. The relative differences observed between the activities of Mo_2C and W_2C for each halobenzene are consistent with metal–halogen enthalpies of formation (ΔH_f°). Assuming the HDH mechanism proceeds without formation of a discrete metal–halogen bond, such a formation will decrease the observed activity of the catalyst by blocking the active metal sites. Reported metal–halogen ΔH_f° values are generally greater for tungsten halides at lower oxidation states and decrease with increased oxidation states [42,43]. For example, the ΔH_f° values for WBr and MoBr are 586 and 457 kJ/mol, respectively, and the ΔH_f° for WCl_2 and $MoCl_2$ are −251 and −289 kJ/mol, respectively. However, the ΔH_f° trend observed with the chlorides, bromides and iodides is reversed for WF_6 and MoF_6 with ΔH_f° values of −1722 and −1586 kJ/mol, respectively. A similar relation between W and Mo fluorides at lower oxidation states could account for the lower activity of W_2C for the HDH of fluorobenzene. This difference is further illustrated in Fig. 5 with the HDH of hexafluorobenzene at 350 °C over the sonochemically prepared catalysts, where the rate of HDH over Mo_2C is twice that of W_2C with benzene as the major product (>90%).

It has been shown that electron-withdrawing substituents on the phenyl ring inhibit the HDH of

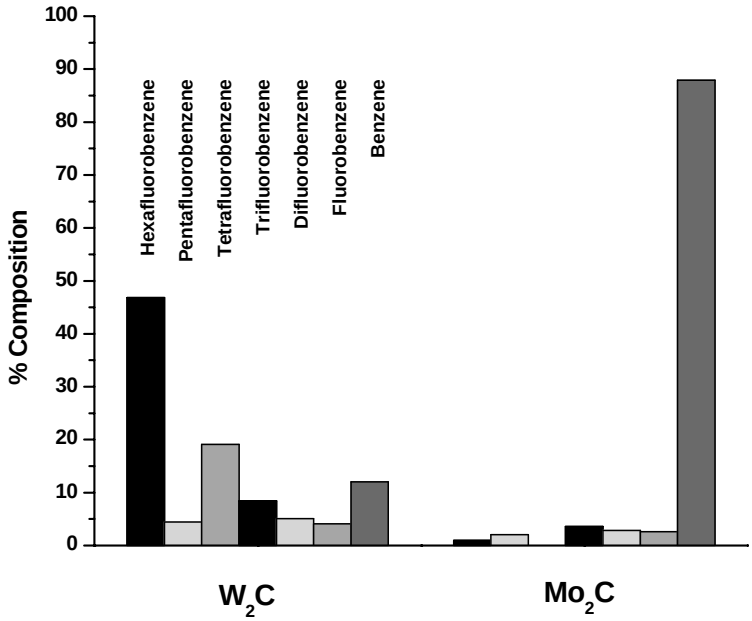

Fig. 5. Catalytic selectivity of Mo_2C and W_2C for the HDH of hexafluorobenzene. Conditions: 350 °C, $P_{H_2}/P_{substrate} = 200{:}1$, and space velocity = 16,500 h^{-1}.

chlorobenzenes over Ni catalysts [40]. Our initial attempt to investigate the effect of various substituents on the HDH of chlorobenzene over sonochemically prepared Mo_2C led to unexpected but interesting observations. Table 1 shows the reaction rate and Fig. 6 shows the selectivity observed when *p*-chloro-α,α,α-trifluorotoluene was examined as a substrate under identical conditions as those used for chlorobenzene. It can be readily noted that the rate is similar to that observed with non-substituted chlorobenzene. The high selectivity for the initial production of *p*-chlorotoluene shows that the hydrogenolysis of the $C_{benzylic}$–F bond is more facile than that of the C_{arene}–Cl bond. This was confirmed by examining the HDH of α,α,α-trifluorotoluene over sonochemical Mo_2C. The serendipitous observation of C–F bond activation by sonochemical Mo_2C under HDH conditions prevents mechanistic evaluation of the electronic effects of electron-withdrawing substituents on chlorobenzene HDH.

Fig. 7 shows the rate and selectivity of CFC-12 HDH at 275 and 325 °C over Mo_2C. The rates increase with temperature and the selectivity is temperature independent. Methane is the major product observed at all temperatures. Unlike conventionally prepared W_2C catalysts, which do not activate C–F bonds in CFC-12 HDH [44], the hydrogenolysis of C–F bonds is observed together with C–Cl bond activation when the HDH of CFC-12 is performed over the sonochemically prepared Mo_2C. The HDH of CFC-22 was also investigated and results in a spectrum of partially dehalogenated hydrocarbons. Methane was observed as the major (>75%) product together with fluoromethane, difluoromethane, chloromethane and chlorofluoromethane. This selectivity to methane is different to that observed over conventionally prepared W_2C, which results in CH_2CF_2 (CFC-32) as the major product [44]. Halogen-exchange products such as CHF_3 or $CHCl_3$ were not observed in these studies. Detailed comparisons of selectivity cannot be made, however, without further studies of the effects of temperature and H_2 concentration, for example, to optimize the catalytic process for the production of hydrofluorocarbons (HCFs) [24].

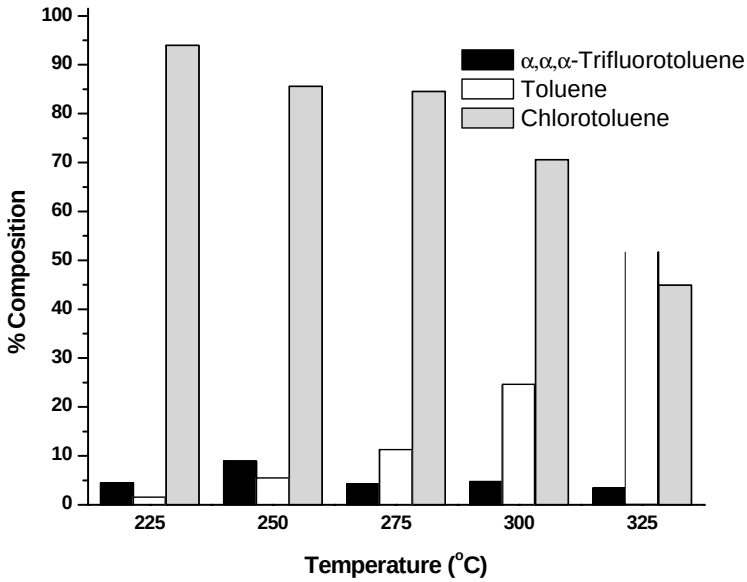

Fig. 6. Catalytic selectivity of Mo_2C for the HDH of *p*-chloro-α,α,α-trifluorotoluene. Conditions: $P_{H_2}/P_{substrate} = 200{:}1$ and space velocity = 16,500 h^{-1}.

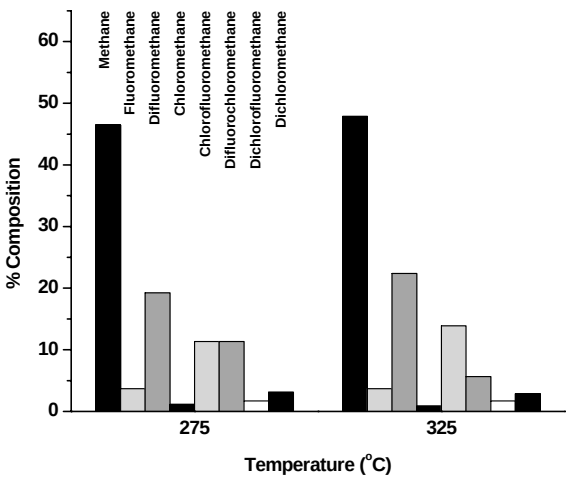

Fig. 7. Catalytic selectivity of sonochemically prepared Mo_2C for the HDH of CFC-12. Conditions: $P_{substrate}/P_{H_2} = 1{:}9$ and space velocity = 16,500 h^{-1}.

3.3. Mechanistic considerations

The activity of sonochemically prepared Mo_2C for non-CFC $C_{aliphatic}$–Cl bond hydrogenolysis was investigated using chlorocyclohexane, 1-chlorobutane, and 1-chloropropane under experimental conditions similar to those used for chlorobenzene. As can be seen from Table 1, the HDH rate for chlorocyclohexane is at least an order of magnitude faster than that observed for the halobenzenes. Previous studies conducted in this laboratory have shown that cyclohexane is readily dehydrogenated to benzene over the sonochemical Mo_2C at temperatures comparable to those of the current studies. Thus, it was anticipated that the HDH of chlorocyclohexane would lead to cyclohexane, which could be dehydrogenated by the same catalyst to benzene. However, neither cyclohexane nor benzene was observed by GC–MS; instead, methylcyclopentane, which is formed presumably via isomerization of a surface bound cyclohexyl intermediate, was the only product observed. The isomerization of cyclohexyl cation to methylcyclopentyl cation under acidic conditions has been previously observed and could account for the formation of the observed methylcyclopentane [45].

In the present study it is predicted that metal carbide-proton adducts may be formed in close proximity to the hydrogenation/dehydrogenation sites. This could lead to "collapsed bifunctional sites", as previously proposed by Sachtler [46,47] and Demirci and Garin [48], on which rapid C–Cl bond hydrogenolysis and alkyl cation isomerization to the most stable

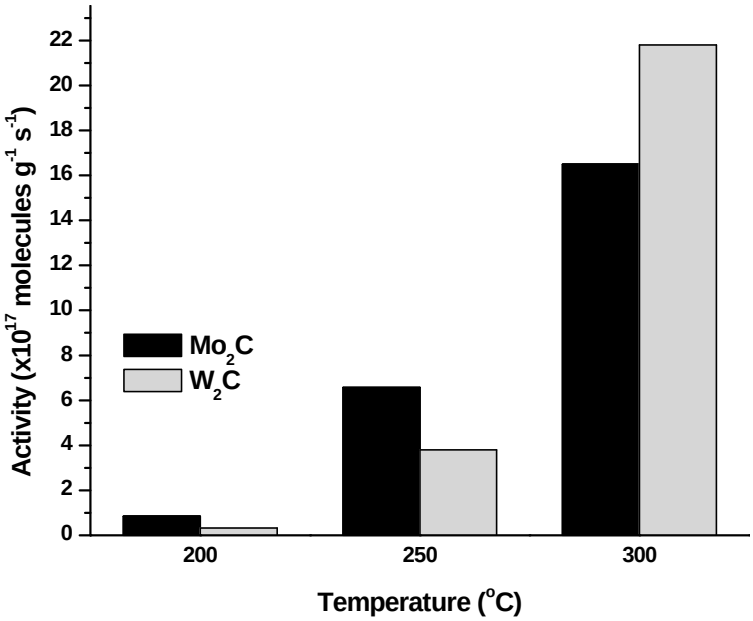

Fig. 8. Catalytic activity of W_2C for the HDH of 4,4′-dichlorobiphenyl. Conditions: 34 atm H_2 and 0.1 M 4,4′-dichlorobiphenyl.

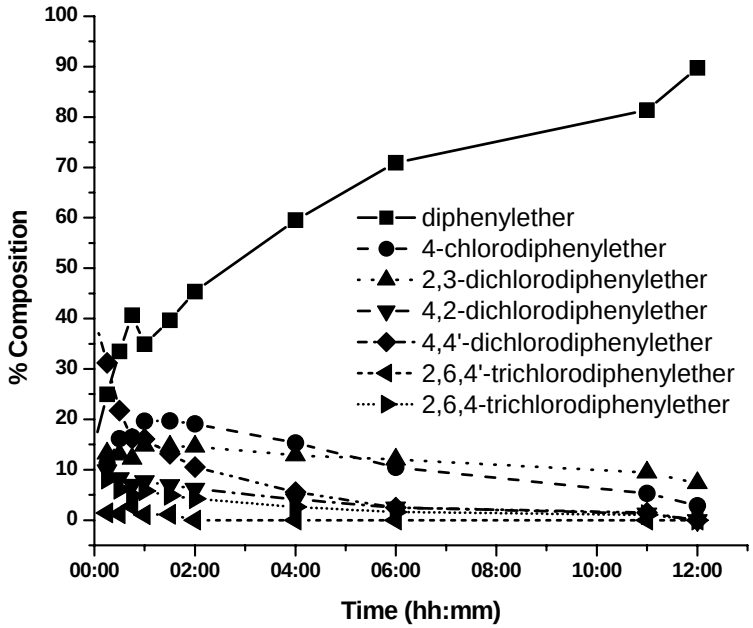

Fig. 9. Catalytic selectivity of W_2C during the HDH of polychlorodiphenylether. Conditions: 34 atm H_2, 0.1 M polychlorodiphenylether, and 300 °C.

cation could occur. Based on previous work by Maire and co-workers [49], oxide impurities from the sonochemical preparation of our catalysts could also contribute to the formation of these acidic bifunctional sites. The observed selectivity to methylcyclopentane suggests that the primary reaction intermediate in the HDH of chlorocyclohexane is a metal-bound secondary cyclohexyl cation, which isomerizes to the more stable methylcyclopentyl tertiary carbocation.

In order to confirm the validity of the above argument, the HDH of 1-chlorobutane was performed under similar conditions. This rate is about five times higher than that observed for chlorobenzene. Isobutane and the dehydrogenated products 1-butene and *cis*- and *trans*-2-butene were the only products detected by GC–MS. The formation of isobutane, presumably via the well-known facile isomerization of the primary butyl cation to the tertiary butyl cation, is consistent with the production of methylcyclopentane from chlorocyclohexane discussed above [50]. The HDH of chloropropane is at least five times faster than that of chlorobenzene and yields a mixture of propane and propene with propene being the major (>80%) product. This observation is in line with the relatively lower $C_{aliphatic}$–Cl bond dissociation energies than those in C_{arene}–Cl [51–53].

3.4. Liquid phase HDH catalysis

Several low volatility substrates were examined in a pressurized batch reactor. Fig. 8 shows the rates for the HDH of 4,4′-dichlorobiphenyl with sonochemically prepared Mo_2C and W_2C. The activity follows the same trend observed with the halobenzenes and the rates are approximately twice that of the gas phase reactions at 300 °C. After 24 h at 300 °C, the primary product is biphenyl (>98%) with small amounts of 4-chlorobiphenyl. The concentration of 4,4′-dichlorobiphenyl was ultimately reduced to <2 ppb. Similar results were observed for the HDH of polychlorodiphenylether, 4,4′-dibromobiphenyl, and 4,4′-dibromodiphenylether. Contrary to the trend observed in the gas phase with chlorobenzene and bromobenzene, the liquid phase HDH rate for 4,4′-dibromobiphenyl, shown in Table 1, is in order of magnitude greater than the HDH rate for 4,4′-dichlorobiphenyl. This liquid-phase trend has also been observed by Aramendia et al. [54] for the

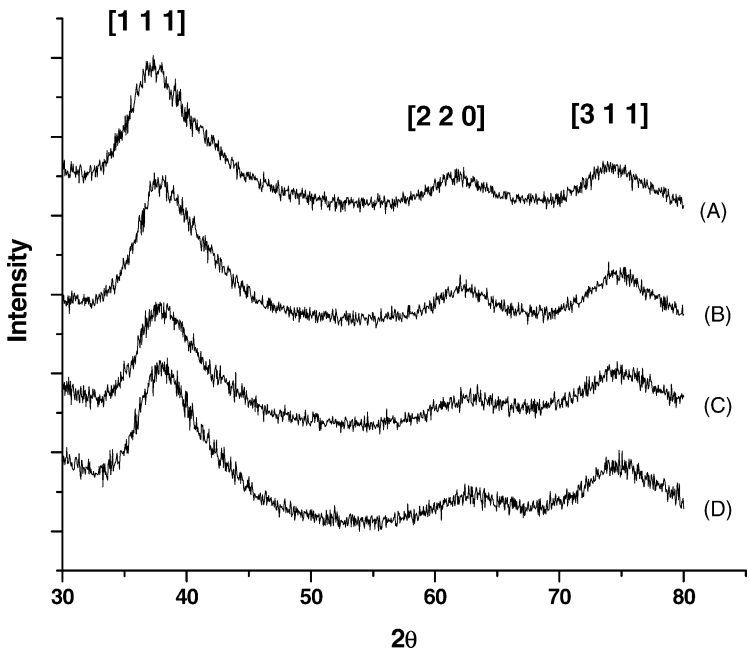

Fig. 10. XRD patters of (A) Mo_2C before catalysis, (B) Mo_2C after catalysis, (C) W_2C before catalysis, and (D) W_2C after catalysis.

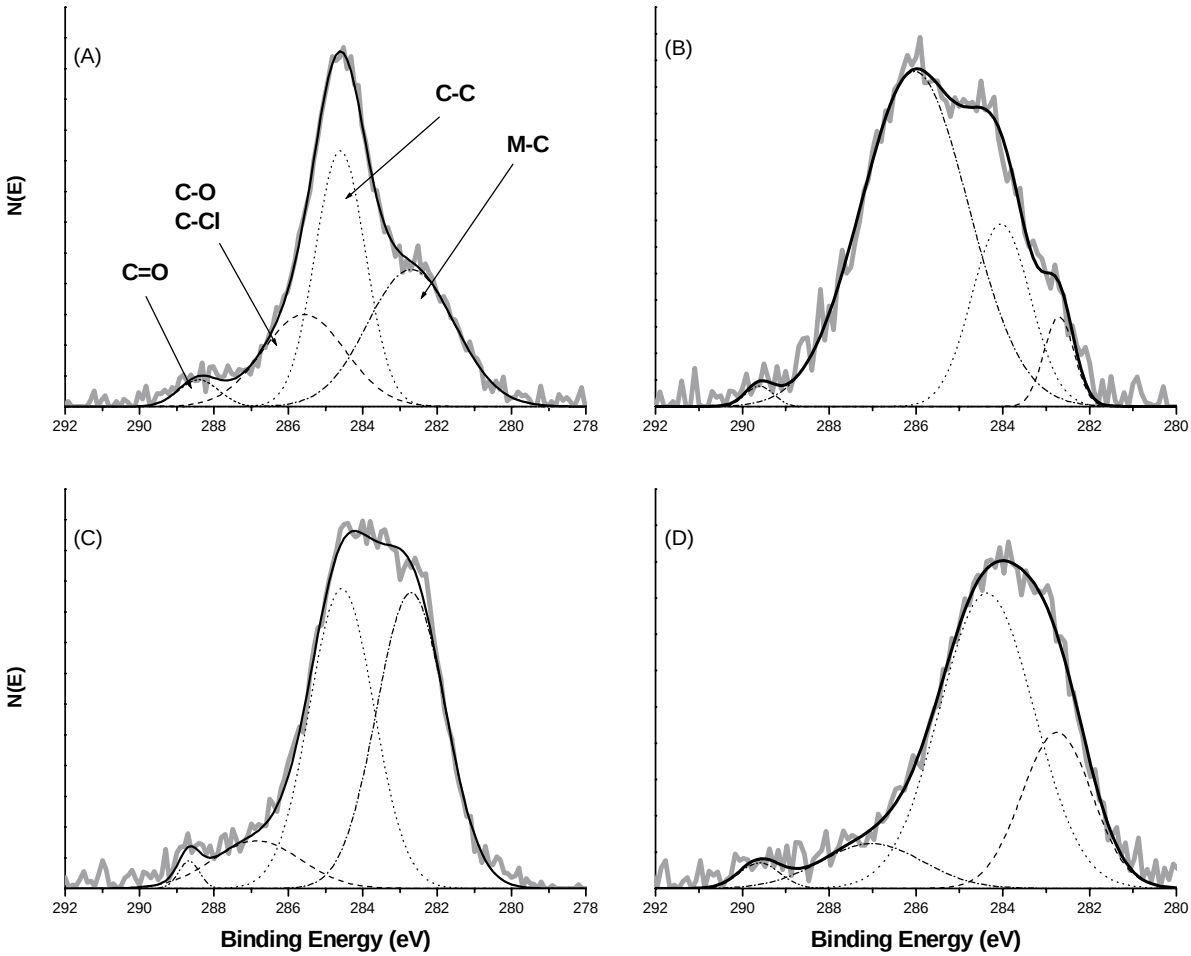

Fig. 11. XPS C1s peak for Mo_2C before (C) and after (A), and W_2C before (D) and after (B). M–C (–·–), C–C (- - -), C–O/C–Cl (– – –), C=O (—).

hydrogenolysis of aryl halides with supported Pd catalysts; it origin, however, warrants further investigation. Although the trend in reactivity differs from gas-phase to liquid-phase, the selectivity remains high. For example, the selectivity for the HDH of polychlorodiphenylether is shown in Fig. 9 and shows diphenylether as the primary product. There was no evidence of hydrogenation of the ring or cleavage of the ether group.

3.5. Effects of HDH on the catalysts

The spent catalysts were analyzed with XPS and XRD using samples from the stability studies shown in Fig. 3. The XRD patterns, shown in Fig. 10, did not change following 100 h of HDH at 300 °C, indicating the catalysts retained their carbide phase and crystallite size. Based on XPS analysis, however, the surface structure and composition exhibited a substantial change. The concentration of chlorine detected in the XPS spectra was 8.5 and 6.1 at.% for Mo_2C and W_2C, respectively. The carbon content for Mo_2C increased slightly from 53.6 to 56.1 at.%, while the carbon content on the surface of the W_2C decreased from 52.9 to 49.7 at.%. The deconvoluted C1s peaks for both catalysts are shown in Fig. 11. Prior to catalysis, the C1s peaks of both catalysts are dominated by carbidic (282.7 eV) and polymeric carbon (∼284.3 eV)

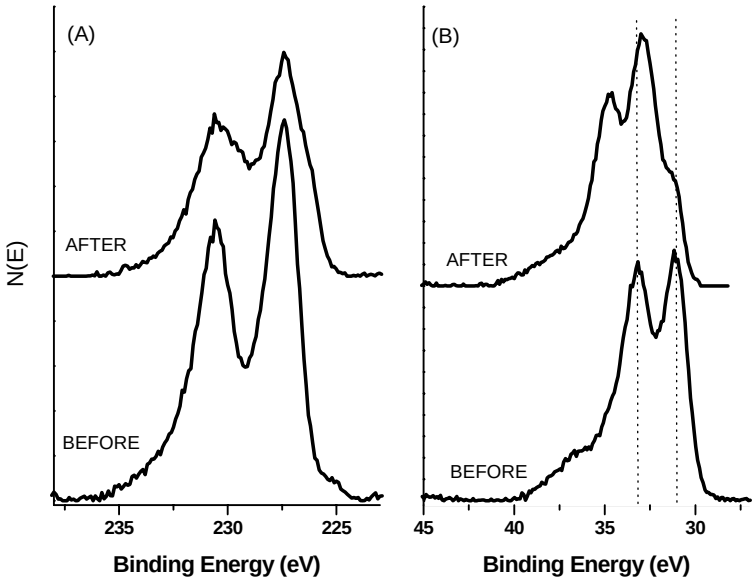

Fig. 12. XPS peaks for (A) Mo ($3d_{5/2}$, $3d_{3/2}$) and (B) W ($4f_{7/2}$, $4f_{5/2}$) after and before catalysis.

with smaller amounts of C–O and C=O. Following 100 h of HDH over Mo_2C, the presence of carbidic carbon and polymeric carbon decrease coupled with an increase in the C–O/C–Cl peak (285.6 eV). This same effect is observed to a greater extent with W_2C. Fig. 12 shows the effect of HDH on the Mo ($3d_{5/2}$, $3d_{3/2}$) and W ($4f_{7/2}$, $4f_{5/2}$) doublets. The doublet for Mo ($3d_{5/2}$, $3d_{3/2}$) is broadened after catalysis due to an average increase in Mo oxidation states as a result of chemisorbed Cl and remains at 227.4 eV. Similar to the C1s, this effect is exaggerated for the W_2C catalyst with a clear shift of the W ($4f_{7/2}$, $4f_{5/2}$) doublet from 31.1 to 33.0 eV.

Due to the absence of any significant increase in polymeric carbon deposits on the surface following catalysis, it is unlikely that coking is the cause of the slight deactivation observed in Fig. 3. The increased presence of higher oxidation states indicates possible chlorination of the surface. This is in agreement with previous explanations offered by Oyama and Giraudon [23,24].

4. Conclusion

In summary, we have demonstrated that sonochemically prepared Mo_2C and W_2C are active, stable, and selective catalysts for the HDH of halogenated organic compounds in both gas and liquid phases. The catalysts are active for CFCs, PCBs, and their analogs. Halogenated aliphatics are catalyzed at a higher rate than halogenated aromatics, and the gas phase trend for the halogenated aromatics is $C_6H_5F > C_6H_5Cl > C_6H_5Br > C_6H_5I$. Results from the HDH of chlorocyclohexane and 1-chlorobutane indicate that the HDH process of sonochemically prepared Mo_2C and W_2C proceeds via a carbenium rather than a radical mechanism. Surface analysis indicates the slow deactivation of the catalyst is a result of surface halogenation rather than coking.

Acknowledgements

The National Science Foundation (CHE-00-79124) and the US Department of Energy (DEFG02-91ER45439) supported this work. Microscopic analyses were carried out at the UIUC Center for Microanalysis of Materials with the support of the Department of Energy through the Frederick Seitz Materials Research Laboratory under contract number DEFG02-91ER45439. The assistance of Drs. Rick Haash and Vania Petrova of the Center for Microanalysis of Materials is appreciated.

References

[1] M.J. Molina, F.S. Rowland, Nature 810 (1974) 474.
[2] L.W. Robertson, L.G. Hansen (Eds.), PCBs: Recent Advances in Environmental Toxicology and Health Effects, The University Press of Kentucky, Lexington, 2001.
[3] M. Alaee, R.J. Wenning, Chemosphere 46 (2002) 579.
[4] P. Eriksson, E. Jakobsson, A. Fredriksson, Environ. Health Perspect. 109 (2001) 903.
[5] C. Schubert, Sci. News 160 (2001) 238.
[6] B. Chen, R.L. Cook, J.D. Wright, in: R.A. Meyers, D.K. Dittrick (Eds.), Encyclopedia of Environmental Pollution and Cleanup, vol. 1, Wiley, New York, 1999, 319 pp.
[7] G. Soderstrom, S. Marklund, Environ. Sci. Technol. 36 (2002) 1959.
[8] K. Olie, P.L. Vermeulen, O. Hutzinger, Chemosphere 8 (1977) 455.
[9] H.R. Buser, H.P. Bosshardt, C. Rappe, Chemosphere 2 (1978) 165.
[10] H.K. Chagger, A. Kendall, A. McDonald, M. Pourkashanian, A. Williams, Appl. Energy 60 (1998) 101.
[11] H. Hagenmaier, M. Kraft, H. Brunner, R. Haag, Environ. Sci. Technol. 21 (1987) 1080.
[12] L.P. Brzuzy, R.A. Hites, Environ. Sci. Technol. 30 (1996) 1797.
[13] J. Corella, J.M. Toledo, Ind. Eng. Chem. Res. 41 (2002) 1171.
[14] B. Coq, G. Ferrat, F. Figueras, J. Catal. 101 (1986) 434.
[15] R.J. Harper, C. Kemball, Trans. Faraday Soc. 65 (1969) 2224.
[16] B. Coq, G. Ferrat, F. Figueras, React. Kinet. Catal. Lett. 27 (1985) 157.
[17] S.T. Srivanas, L.J. Lakshmi, N. Lingaiah, P.S. Sai Prasad, P. Kanta Rao, Appl. Catal. A 135 (1996) L201.
[18] E.J. Creyghton, M.H.W. Burgers, J.C. Jansen, H. van Bekkum, Appl. Catal. A 128 (1995) 275.
[19] H.C. Choi, S.H. Choi, J.S. Lee, K.H. Lee, Y.G. Kim, J. Catal. 166 (1997) 284.
[20] N. Lingaiah, M.A. Uddin, A. Muto, T. Iwamoto, Y. Sakata, Y. Kusano, J. Mol. Catal. A 161 (2000) 157.
[21] C. Menini, C. Park, E.J. Shin, G. Tavoularis, M.A. Keane, Catal. Today 62 (2000) 355.
[22] F. Murena, E. Schioppa, Appl. Catal. B 27 (2000) 257.
[23] B. Dhandapani, S.T. Oyama, Catal. Lett. 35 (1995) 353.
[24] L. Delannoy, J.M. Giraudon, P. Granger, L. Leclercq, G. Leclercq, Catal. Today 59 (2000) 231.
[25] K.S. Suslick, in: G. Ertl, H. Knozinger, J. Weitkamp (Eds.), Handbook of Heterogeneous Catalysis, vol. 3, Wiley-VCH, Weinheim, 1997, p. 1350.
[26] K.S. Suslick, G.J. Price, Annu. Rev. Mater. Sci. 29 (1999) 295.
[27] N.A. Dhas, A. Ekhtiarzadeh, K.S. Suslick, J. Am. Chem. Soc. 123 (2001) 8310.
[28] G. Danstin, K.S. Suslick, J. Am. Chem. Soc. 122 (2000) 5214.
[29] K.S. Suslick, L.A. Crum, in: M.J. Crocker (Ed.), Encyclopedia of Acoustics, vol. 1, Wiley-Interscience, New York, 1997, p. 271.
[30] W.B. McNamara, Y.T. Didenko, K.S. Suslick, Nature 401 (1999) 772.
[31] T.H. Hyeon, M.M. Fang, K.S. Suslick, J. Am. Chem. Soc. 118 (1996) 5492.
[32] L.A. Crum, T.J. Mason, J.L. Reisse, K.S. Suslick (Eds.), Sonochemistry and Sonoluminescence, Kluwer Academic Publishers, Dordrecht, 1999.
[33] E.B. Flint, K.S. Suslick, Science 253 (1991) 1397.
[34] JCPDS card number 15-457.
[35] JCPDS card number 20-1316.
[36] H.P. Klug, L.E. Alexander, X-ray Diffraction Procedures for Polycrystalline and Amorphous Materials, Wiley, New York, 1974.
[37] M.J. Ledoux, C.P. Huu, J. Guille, H. Dunlop, J. Catal. 134 (1992) 383.
[38] J.S. Lee, M.H. Yeom, K.Y. Park, I.S. Nam, J.S. Chung, Y.G. Kim, S.H. Moon, J. Catal. 128 (1991) 126.
[39] E.J. Shin, M.A. Keane, Chem. Eng. Sci. 54 (1999) 1109.
[40] A.R. Suzdorf, S.V. Morozov, N.N. Anshits, S.I. Tsiganova, A.G. Anshits, Catal. Lett. 29 (1994) 49.
[41] C. Park, C. Menini, J.L. Valverde, M.A. Keane, J. Catal. 211 (2002) 451.
[42] W.E. Dasent, Inorganic Energetics, 2nd ed., Cambridge University Press, Cambridge, 1970, p. 185.
[43] M.W. Chase Jr., J. Phys. Chem. Ref. Data 9 (1998) 1.
[44] F.G. Sherif, US Patent 5,426,252 (1995).
[45] M. Saunders, J. Rosenfeld, J. Am. Chem. Soc. 91 (1969) 7756.
[46] W.M.H. Sachtler, Acc. Chem. Res. 26 (1993) 383.
[47] X. Bai, W.M.H. Sachtler, J. Catal. 129 (1991) 266.
[48] U.B. Demirci, F. Garin, J. Mol. Catal. A 188 (2002) 233.
[49] V. Keller, P. Wehrer, F. Garin, R. Ducrox, G. Maire, J. Catal. 166 (1997) 125.
[50] G. Olah, J. Lukas, J. Am. Chem. Soc. 89 (1967) 2227.
[51] S.W. Benson, J. Chem. Phys. 29 (1958) 546.
[52] S.W. Benson, Thermochemical Kinetics, 2nd ed., Wiley, New York, 1976.
[53] D.R. Lide, Handbook of Chemistry and Physics, CRC Press, Boca Raton, 1993.
[54] M.A. Aramendia, V. Borau, I.M. Garcia, C. Jimenez, A. Marinas, J.M. Marinas, F.J. Urbano, C.R. Acad. Sci., Ser. IIc 3 (2000) 465.